

PAPER DETAILS

TITLE: MODIFIED HIGH STEP-UP COUPLED INDUCTOR BASED DC-DC CONVERTER FOR PV APPLICATIONS

AUTHORS: N RAMESH BABU,S SARAIVANAN

PAGES: 981-986

ORIGINAL PDF URL: <https://dergipark.org.tr/tr/download/article-file/273174>



Modified High Step-Up Coupled Inductor based DC-DC Converter for PV Applications

S. SARAVANAN¹, N. Ramesh BABU^{1, *}

¹ School of Electrical Engineering, VIT University, Vellore, Tamil nadu, India

Received: 05/08/2016

Accepted: 20/09/2016

ABSTRACT

A modified high voltage gain dc-dc converter with improved efficiency has been proposed in this article for PV based applications. In the proposed methodology, converter is integrated with a switched capacitor and a switched coupled inductor. This converter topology provides high voltage gain with fewer components. The efficient power conversion has been achieved with low switching voltage across the semiconductor devices. The working principle and analysis of the converter are described in this article. The converter design is made for 250-W power rating system. Performance of the proposed converter is analysed and validated the efficiency at various loading conditions.

Keywords: dc-dc converter, high voltage gain, switched capacitor, coupled inductor, switching voltage, photovoltaic.

1. INTRODUCTION

The high voltage gain dc-dc isolated converter is mainly used for renewable energy system. Non conventional power conversion system plays major role in recent years. This type of generating system produces the energy in environmental and naturally available sources. Renewable energy sources namely wind energy, photovoltaic (PV) [1-3] and fuel cell systems are mostly preferred for the generating power [4-6]. The research on PV based power generation was tremendously increased in recent years. The main advantage of the PV system is its easy installation and non polluted power generation. The maximum power is harvested from the PV system by

using Maximum Power Point Tracking (MPPT) techniques [7-9]. MPPT algorithms were deployed to track the optimum point from the PV characteristics. The generating voltage from the PV system is low and hence an appropriate converter has been utilized for boosting up the voltage as per the requirement of the system application.

*Corresponding author, e-mail: nrameshbabu@vit.ac.in

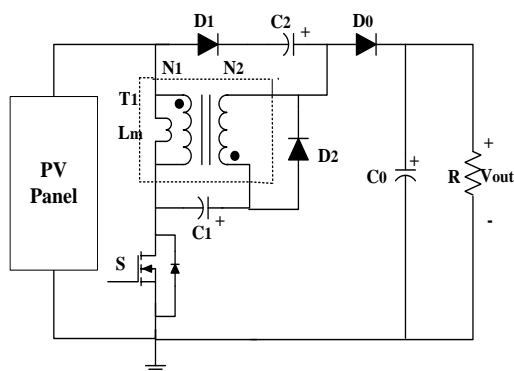


Figure 1. Circuit diagram of the proposed converter.

The classical boost converter topology is not sufficient to produce high voltage gain even with large duty cycle value. As the design aims large duty cycle value, the reverse recovery and electromagnetic interference issues will occur in the converter output [10]. Hence the classical converter efficiency gets reduced even in the low power application. Alternately, many papers are proposed with high step up dc-dc converters [11-22], which have large input current and high output voltages. The high inrush current passes to the system introduces high voltage stress for the switch and diode in the circuit. This reduces the efficiency of the converter due to switching and conduction loss.

The transformer less converters operates using large duty cycle to attain the high voltage gain [11-13]. Some of the other converters in the literature use transformers with flyback and forward converters. These converters reach the high voltage by varying the transformer turn's ratio instead of duty cycle. Due to the presence of leakage inductance in the transformer coil, high voltage stress is developed across the semi-conductor devices [14].

The converter efficiency and high voltage gain was achieved in various converters that are proposed in [15-17]. The coupled inductor methodology is used instead of transformer to obtain the high voltage gain with reduction in the leakage inductance. This introduces voltage spike across the switch and hence the conversion efficiency gets reduced [18, 19]. Combination of boost and fly-back converter was proposed in [20], in which the secondary coil of coupled inductor is used to increase the voltage gain. By adjusting the turn's ratio of coupled inductor the voltage spike of the main switch and stress gets reduced. In [21], converter is designed using the combination of coupled inductor with two multiplier voltage cells to produce high voltage gain and applied for the renewable applications. The energy in the leakage inductor is recycled with the help of passive clamp circuit. Boost interleaved converter [22] is also used for high step voltage operation but the number of switches are high which leads to the conduction loss.

This article proposes a high voltage gain dc-dc isolated converter suitable for PV system to generate the high voltage gain with reduced switching voltage stress. In this proposed converter topology, the reverse recovery losses are avoided. For the system design, PV panel power rating of 250 W with maximum power point voltage of $V_{mpp} = 20$ V is considered. This design uses less components and used for high voltage rating applications.

Compared to fly-back converter, this method has low switching voltage and requires less duty ratio to achieve the high step up voltage gain.

In this manuscript, section 2 describes the operating principle and analysis of the proposed converter. In section 3, the implementation of the proposed converter and the results obtained were discussed. Finally, conclusion is presented in section 4.

2. OPERATING PRINCIPLE AND ANALYSIS OF PROPOSED CONVERTER

The basic circuit diagram of the proposed converter is shown in Fig. 1. It consists of three diodes D1, D2 and D0, capacitor C1, C2 and C0, coupled inductor T1, with single switch S. L_m , magnetizing part of the coupled inductor acts as an input inductor of the converter. Switching capacitor, C2 get the charge from the input supply V_{in} and flows through the secondary winding N2. The output capacitor, C0 will discharge the current to the load resistor R through diode D0.

The proposed converter is operated first with the coupled inductor, and transfers the energy to the switch to turn ON or OFF. In second stage, the energy from the input supply is stored in switched capacitor and secondary side N2 of coupled inductor. The charging current of the switched capacitor C1 was limited by using leakage inductance, which in turn reduces the inrush current flow through the switching capacitor. The charge dissipated in the leakage inductor had been regenerated by coupled inductor and given to the load so as to improve the power conversion efficiency. This reduces the duty ratio in the converter with high voltage gain.

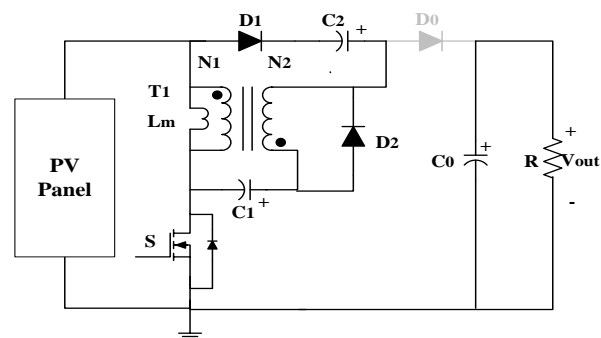


Figure 2. Mode I operation of the proposed converter.

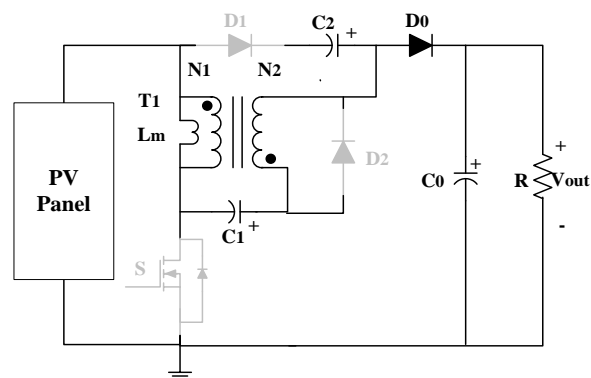


Figure 3. Mode II operation of proposed converter.

2.1. Modes of Operation

The proposed converter operates in two modes of operation under continuous conduction principle as discussed below.

Mode I [t₀, t₁]: When the switch is in ON condition, the diode D1 and D2 conducts and diode D0 gets reverse biased as illustrated in Fig. 2. In this mode, the switched capacitor receives energy from the input supply and coupled inductor. Hence the input current flows from switched capacitor C1 to the diode D1 which is connected series to the secondary side of the coupled inductor. The charges start storing in the magnetizing inductor L_m. The capacitor C0 discharges the energy and flows to the load resistor R.

Mode II [t₁, t₂]: When the switch is in turned OFF condition, the diode D1 and D2 become reverse bias and diode D0 is forward biased as shown in Fig. 3. As the stored charge from the magnetizing inductor L_m starts discharging, the polarity of L_m gets reversed and the diode D0 starts conducting. The current flows from V_{in} input source to the load through the magnetizing inductor L_m, switched capacitor C1, secondary winding N2, diode D0, and the output capacitor C0. During this operation the capacitor C0 starts storing the charge from the diode D0.

The waveforms of continuous conduction mode (CCM) of proposed converter are shown in Fig. 4. In CCM, the leakage inductance of the coupled inductor (primary side) is neglected. The voltage flows in the primary side N1 of the coupled inductor is computed as,

$$V_{N1} = V_{in} \left(\frac{D}{1-D} \right) \quad (1)$$

The secondary side N2 voltage of inductor is n times V_{N1},

$$V_{N2} = V_{in} \left(\frac{nD}{1-D} \right) \quad (2)$$

By using the above equations, it is clear that the number of turns using coupled inductor is small and can able to generate high voltage gain with reduced voltage stress and current stress across the switch.

2.2. Design of Coupled Inductor and Capacitors

The coupled inductor is designed based on the selection of low magnetizing inductance parameter for the converter under CCM mode. The switched capacitor is designed based on the output power level and ripple voltage in capacitor. The magnetizing inductance is obtained, during the boundary conduction mode (BCM) and it is shown as,

$$L_{m(Boundary)} = \frac{R_{oB}(1-D)^2 D}{2(1+2N-ND)(1+N)f_s} \quad (3)$$

$$C_1 = C_2 \geq \frac{I_o(1-D)}{f_s(\Delta V_{C1})(\Delta V_{C2})} \quad (4)$$

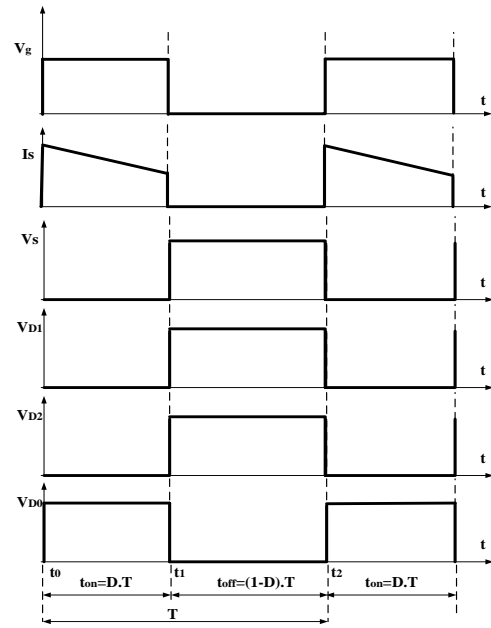


Figure 4. The characteristic waveforms of proposed converter.

where RoB is the boundary condition load, D is the duty cycle, N is the number of turns, I_o is the output current, f_s is the switching frequency, ΔV_{C1} and ΔV_{C2} are the ripple voltage of capacitors. The capacitor value is computed with the assumption of ripple voltage as 26% of the nominal voltage level.

2.3. Steady-State Analysis

Under steady state condition the voltage gain ratio of the modified dc-dc isolated converter proposed with continuous conduction mode (CCM) and discontinuous conduction mode (DCM) is computed using equations (3) and (4).

$$M_{CCM} = \frac{V_o}{V_{in}} = \frac{2-D+n}{1-D} \quad (5)$$

$$M_{DCM} = \frac{D_L D}{2(1+n)\tau_m} \quad (6)$$

Where n is the number of inductor turns, D is the duty cycle, D_L is the time period for reducing the magnetizing current from peak to zero and τ_m is the time constant. Figure 5 shows the plot of voltage gain ratio under CCM condition of the proposed converter with various turns ratio. The time constant based boundary normalised magnetizing-inductance (τ_{LmB}) is given as,

$$\tau_{LmB} = \frac{D(1-D)^2}{2(2+n-D)(1+n)} \quad (7)$$

The τ_{LmB} of the proposed converter under CCM and DCM is shown in Fig. 6. From these analyses, it is observed that the smaller turn ratio is sufficient for magnetizing larger inductance of the coupled inductor.

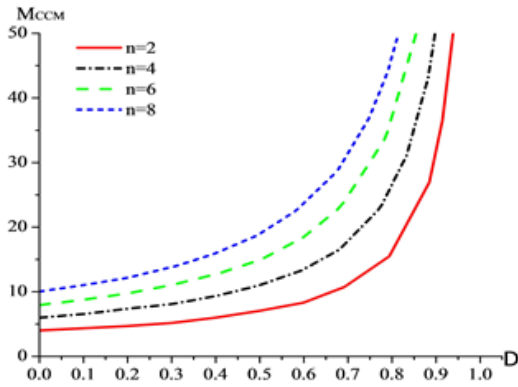


Figure 5. Voltage gain ratio vs duty cycle of the proposed converter under CCM operation with $n=2\sim 8$.

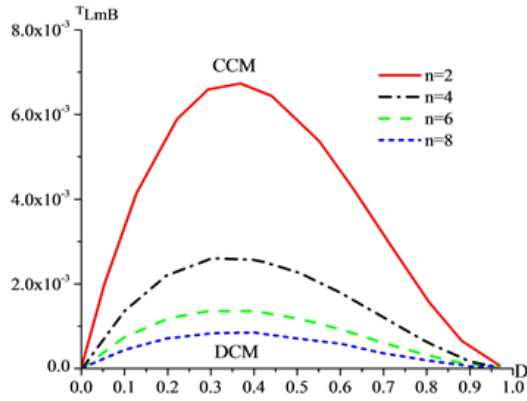


Figure 6. τLmB vs duty cycle of the proposed converter under $n=2\sim 8$.

3. IMPLEMENTATION AND RESULTS

A 250-W PV system has been considered for simulation using MATLAB/Simulink. The parameters used for the simulation study are listed in Table 1. Figure 7, shows the primary winding current, output load current and output voltage of the proposed converter. From Fig. 7, it is observed the proposed converter reaches maximum inductor current of 40 A with the output current and output voltage of 1.18 A and 220 V respectively. Figure 8 shows the duty cycle, voltage and current waveforms of the switch in proposed converter. From the analysis, it is observed that the voltage of the switch is 37 V which is very less than the output voltage (220V) and the switching current is 36 A.

The frequency domain analysis is performed for the proposed converter by deriving its average circuit model as shown in Fig. 9. The switching current is derived from the average current through the switch S and average voltage through diode $D1$, $D2$ and $D0$ can be obtained as,

$$\langle i_s \rangle T_s = G_s = di_{Lm} + \frac{V_o}{R} \quad (8)$$

$$\langle v_{D1} \rangle T_s = E_{D1} = -dv_{C1} \quad (9)$$

$$\langle v_{D2} \rangle T_s = E_{D2} = (1-d)(v_o - v_{C1}) \quad (10)$$

$$\langle v_{D0} \rangle T_s = E_{D0} = d(v_o - v_{C1} - v_{C2}) \quad (11)$$

where, T_s is the switching cycle, i_s is the switching current, v_{D1} , v_{D2} and v_{D0} are the average voltage of diodes, V_o is the output voltage of converter, V_{C1} and V_{C2} are the capacitors voltage. The simulated open-loop small-signal transfer function based output voltage to input voltage is plotted using bode plot [11] as shown in Fig. 10. This analysis is useful to design the controller for the proposed converter circuit.

Table 1: Simulation Parameters.

Output Power	250 W
Input Voltage (V_{in})	20 V
Output Voltage (V_{out})	220 V
Switching Frequency (f_s)	50 KHz
Duty Cycle	0.5
Coupled Inductor ($N_1:N_2$)	1:2
Magnetizing Inductor (L_m)	23 μ H
Capacitor (C_1)	100 μ F
Capacitor (C_2)	25 μ F
Capacitor (C_0)	10 μ F
Resistor	193.6 Ω
Voltage Gain	11

From the waveforms, it can be observed that the voltage and current stress of the semiconductor devices are low in the proposed converter. The efficiency of the proposed converter versus output power is shown in Fig. 11. This figure reveals that for lighter load, the efficiency is very high of 97.5 % and it drops gradually to 93.8 % for the full load, 250 W so as to maintain the constant designed voltage of 220 V.

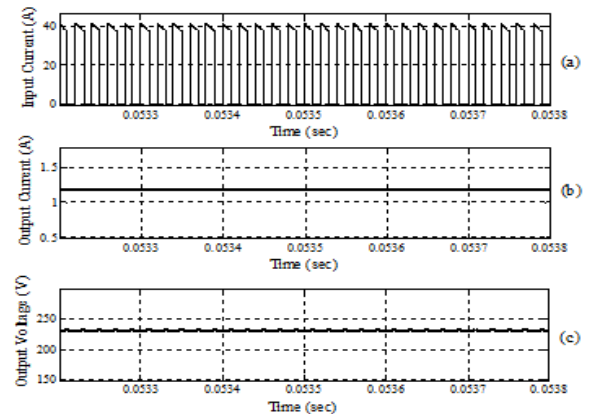


Figure 7. The waveforms of the proposed converter- (a) input current, (b) output current and (c) output voltage.

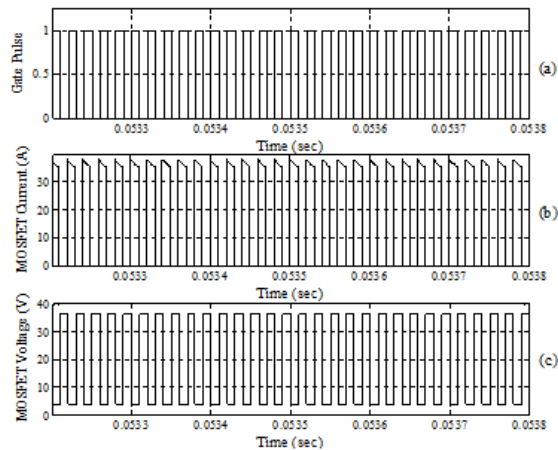


Figure 8. The waveforms of the proposed converter- (a) switch duty cycle, (b) switch current and (c) switch voltage.

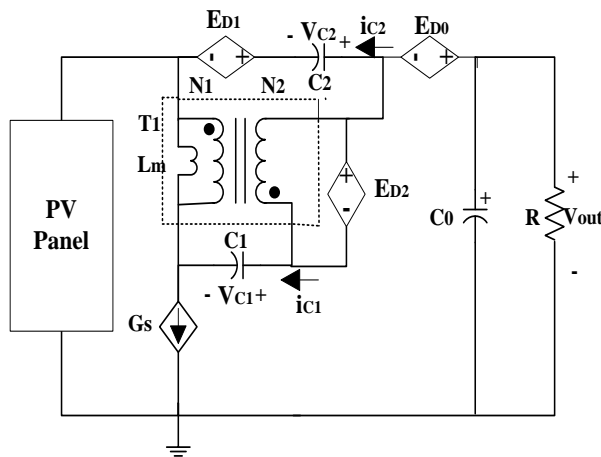


Figure 9. Average circuit model for the proposed converter.

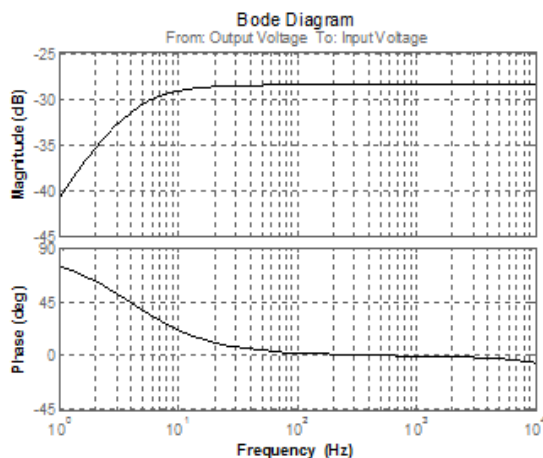


Figure 10. Open-loop small-signal frequency responses of proposed converter.

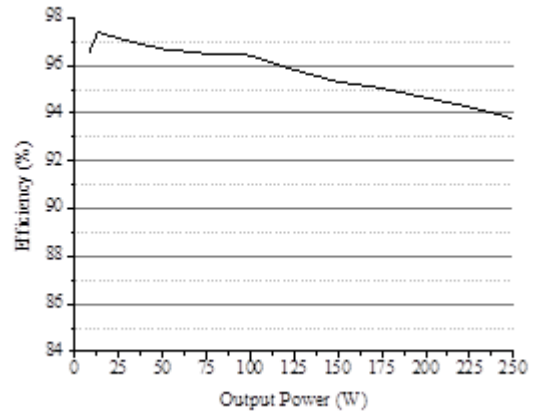


Figure 11. Efficiency curve of the proposed converter.

4. CONCLUSION

This paper describes the design of modified high voltage gain dc-dc converter with reduced voltage stress across the switch. The CCM and DCM of converter operation have been analysed with various turn ratio to identify the effect of magnetising inductance. By utilizing the switched capacitor and coupled inductor the high voltage conversion ratio is achieved by the proposed converter. The proposed converter is validated using MATLAB/Simulink platform. The simulation result shows that the performance of the proposed converter reaches a maximum of 93.8 % at full load (250 W) conditions. Also, the frequency domain analysis of the proposed converter is done by developing the small signal circuit and the Bode plot response. The low rating components are used for the proposed converter which reduces the system cost. This proposed converter finds a lot of importance in the PV based power generation applications.

ACKNOWLEDGEMENTS

Authors would like to thank School of Electrical Engineering, VIT University for providing the required support to successfully carry out this study.

CONFLICT OF INTEREST

No conflict of interest was declared by the authors.

REFERENCES

- [1] Saravanan, S. and Babu, N.R. "Maximum power point tracking algorithms for photovoltaic system – A review," *Renew. & Sustain. Energy Rev.*, vol. 57, pp. 192-204. (2016).
- [2] Ramji Tiwari, and Babu, N.R, "Fuzzy Logic Based MPPT for Permanent Magnet Synchronous Generator in wind Energy Conversion System", *IFAC-PapersOnLine*, vol. 49, no. 1, pp. 462-467, (2016).

- [3] Saravanan, S. and Babu, N.R., "Performance analysis of boost and cuk converter in MPPT based PV system," In: Proceedings of the Inter Conference on Circuit, Power and Comput Technol, pp. 1-6, (2015).
- [4] Li, Y., Vilathgamuwa, D.M. and Loh P.C. "Design, analysis, and realtime testing of a controller for multibus microgrid system," IEEE Trans. Power Electron., vol. 19, no. 5, pp. 1195-1204, (2004).
- [5] Timbus, A., Liserre, M., Teodorescu, R., Rodriguez, P., and Blaabjerg, F. "Evaluation of current controllers for distributed power generation systems," IEEE Trans. Power Electron., vol. 24, no. 3, pp. 654–664, (2009).
- [6] Mohamed, Y.A-R.I. and El Saadany, E. F. "Adaptive decentralized droop controller to preserve power sharing stability of paralleled inverters in distributed generation microgrids," IEEE Trans. Power Electron., vol. 23, no. 6, pp. 2806–2816, (2008).
- [7] Sivakumar, P., Kader, A.A., Kaliavaradhan, Y., and Arutchelvi, M. "Analysis and enhancement of PV efficiency with incremental conductance MPPT technique under non-linear loading conditions," Renew. Energy, vol. 81, pp. 543-550, (2015).
- [8] Kofinas, P., Dounis, Al., Papadakis, G., and Assimakopoulos, M.N. "An intelligent MPPT controller based on direct neural control for partially shaded PV system," Energy and Build. vol. 90, pp. 51-64, (2015).
- [9] Qi, J., Zhang, Y., and Chen, Y. "Modeling and maximum power point tracking (MPPT) method for PV array under partial shade conditions," Renew. Energy. vol. 66, pp. 337-345, (2014).
- [10] Wai, R.J., Lin, C.Y., Duan, R.Y., and Chang, Y.R. "High efficiency power conversion system for kilowatt-level stand-alone generation unit with low input voltage," IEEE Trans. Ind. Electron., vol. 55, no. 10, pp. 3702–3714, (2008).
- [11] Saravanan, S. and Babu, N.R. "RBFN based MPPT algorithm for PV system with high step up converter," Energy Convers. and Manag., vol. 122, pp. 239-251, (2016).
- [12] Gules. R., dos Santos, W.M., dos Reis, F.A. Romaneli, E.F.R., and Badin, A.A. "A Modified SEPIC converter with high static gain for renewable applications," IEEE Trans. Power Electron., vol. 29, no. 11, pp. 5860–5871, (2014).
- [13] Sabzali, A.J., Ismail, E.H., and Behbehani, M. "High voltage step-up integrated double Boost-Sepic DC-DC converter for fuel-cell and photovoltaic applications," Renew. Energy, vol. 82, pp. 44-53, (2015).
- [14] Carr, J.A., Hotz, D., Balda, J.C., Mantooth, H.A., Ong, A., and Agarwal, A. "Assessing the impact of SiC MOSFETs on converter interfaces for distributed energy resources," IEEE Trans. Power Electron., vol. 24, no. 1, pp. 260–270, (2009).
- [15] Lin, B.R. and Hsieh, F.Y. "Soft-switching zeta-flyback converter with a buck-boost type of active clamp," IEEE Trans. Ind. Electron., vol. 54, no. 5, pp. 2813–2822, (2007).
- [16] Wu, T.F., Lai, Y.S., Hung, J.C., and Chen, Y.M. "Boost converter with coupled inductors and buck-boost type of active clamp," IEEE Trans. Ind. Electron., vol. 55, no. 1, pp. 154–162, (2008).
- [17] Wai, R.J., Liu, L.W., and Duan, R.Y. "High-efficiency voltage-clamped dc-dc converter with reduced reverse-recovery current and switch voltage stress," IEEE Trans. Ind. Electron., vol. 53, no. 1, pp. 272–280, (2006).
- [18] Zhao, Q., and Lee, F.C. "High-efficiency, high step-up DC-DC converters," IEEE Trans. Power Electron., vol. 18, no. 1, pp. 65–73, (2003).
- [19] Chen, S.M., Lao, M.L., Hsieh, Y.H., Liang, T.J., and Chen, K.H. "A Novel Switched -Coupled-Inductor DC-DC Step-Up converter and Its Derivatives," IEEE Trans. Ind. App., vol. 51, no. 1, pp. 309-314, (2015).
- [20] Chen, Z., Zhou, Q., and Xu, J., "Coupled-inductor boost integrated flyback converter with high-voltage gain and ripple-free input current," IET Power Electron., vol. 8, no. 2, pp. 213-220, (2015).
- [21] Ajami, A., Ardi, H., and Farakhori, A. "A Novel High Step-up DC/DC Converter Based on Integrating Coupled Inductor and Switched-Capacitor Techniques for Renewable Energy Applications," IEEE Trans. Power Electron, vol. 30, no. 8, pp. 4255–4263, (2015).
- [22] Aquino, R.N.A.L.S., Tofoli, F.L., Praca, P.P., Jr, D.S.O., and Barreto, L.H.S.C. "Soft switching high-voltage gain dc-dc interleaved boost converter," IET Power Electron, vol. 8, no. 1, pp. 120-129, (2015).